JOURNAL OF GEOPHYSICAL RESEARCH, VOL. 96, NO. B6, PAGES 9937–9946, JUNE 10, 1991

Slaty Cleavage Development and Magnetic Anisotropy Fabrics

BERNARD A. HOUSEN AND BEN A. VAN DER PLUIJM

Department of Geological Sciences, University of Michigan, Ann Arbor

The shale-to-slate transition preserved in the Ordovician Martinsburg Formation at the Lehigh Water Gap, Pennsylvania, provides an opportunity to study the relationship between magnetic anisotropy fabrics and the development of slaty cleavage. Our previous work has indicated that anisotropy of magnetic susceptibility (AMS) does not record changes in finite strain associated with cleavage development in these rocks but instead measures the degree of dissolution and new growth of chlorite. Additional AMS data presented in this paper lend further support to this conclusion. Conversely, anhysteretic remanent magnetization anisotropy (ARMA), which is not affected by paramagnetic chlorite, accurately reflects the strain-induced rock fabrics associated with cleavage formation. ARMA results show that magnetite dimensional orientations vary from bedding-parallel in shale samples to cleavage-parallel in samples with well-developed slaty cleavage. Samples with weak and pencil cleavage display scattered ARMA orientations which lie in between bedding and cleavage. These intermediate orientations may be due to either passive rotation of magnetite from bedding-parallel to cleavage-parallel or (re)crystallization of magnetite. If rotation occurred, grain rotation was highly heterogeneous in the samples with incipient cleavage. The intermediate ARMA orientations may also reflect the varying contribution of two magnetite preferred orientations, a depositional orientation parallel to bedding and a new growth orientation parallel to cleavage.

INTRODUCTION

Magnetic anisotropy has been utilized by many workers in a variety of geological and geophysical applications. Early work focused on possible deflection of natural remanent magnetization (NRM) directions by anisotropy of ferrimagnetic minerals, as measured by the anisotropy of magnetic susceptibility (AMS) [*Fuller*, 1963]. *Girdler* [1961] demonstrated that the anisotropy of magnetic susceptibility could be described as a second-order tensor, and that this tensor defines the susceptibility ellipsoid, with maximum (k_{max}), intermediate (k_{int}) and minimum (k_{min}) principal axes having both magnitude and direction. AMS in individual minerals reflects either a shape anisotropy, with k_{max} parallel to the long-dimension of the mineral and k_{min} parallel to the short dimension, or a crystalline anisotropy in which the AMS axes are associated with the crystallographic axes. In phyllosilicates for example, k_{min} is generally parallel to the *c* - axis and k_{max} and k_{int} lie in the basal plane. AMS thus has the potential to measure dimensional or crystallographic preferred orientations of minerals in a rock.

Many early studies of the anisotropy of magnetic susceptibility successfully correlated the orientation of the susceptibility ellipsoid with mesoscopic rock fabrics, such as bedding or cleavage [*Graham*, 1954; *Fuller*, 1963; *Uyeda et al.*, 1963; *Singh et al.*, 1975]. More recent efforts have concentrated on correlations between the AMS ellipsoid and the finite strain ellipsoid [*Owens*, 1974; *Hrouda*, 1976, 1980, 1987; *Wood et al.*, 1976; *Kligfield et al.*, 1977; *Rathore*, 1979, 1988; *Borradaile and Tarling*, 1981; *Henry and Daly*, 1983; *Borradaile and Mothersill*, 1984; *Borradaile*, 1987; *Borradaile and Alford*, 1987, 1988; *Cogne and Perroud*, 1988; *Goldstein and Brown*, 1988; *Hirt et al.*, 1988, *Hrouda and Lanza*, 1989; *Vetter et al.*, 1989; *Bossart et al.*, 1990]. These studies have generally determined that the finite strain and susceptibility ellipsoids are coaxial in orientation, but attempts to correlate the magnitudes of the finite strain ellipsoid and the AMS ellipsoid have met with mixed success (see review by *Borradaile*, [1988]). Questions arising from these efforts have led to studies that have revealed the complex nature of AMS in rocks [*Rochette and Vialon*, 1984; *Borradaile et al.*, 1986, 1987; *Pearce and Fueten*, 1989]. While ferrimagnetic minerals such as magnetite were originally thought to control the AMS in rocks, recent work has shown that the contribution of paramagnetic and diamagnetic matrix minerals, such as chlorite and calcite, to the measured AMS can exceed that of the ferrimagnetic minerals [*Rochette*, 1987; *Hrouda et al.*, 1988; *Henry*, 1989; *Jackson et al.*, 1989; *Jover et al.*, 1989; *Borradaile and Sarvas*, 1990; *Housen and van der Pluijm*, 1990]. Changes in composition or the relative proportions of minerals in a rock, for example the addition of more magnetite [*Johns et al.*, 1990], can also produce variations in the measured AMS. Moreover, certain minerals, such as ferroan calcite, tourmaline, and single-domain magnetite rods, have been found to display anomalous "inverse" AMS fabrics [*Potter and Stephenson*, 1988; *Rochette*, 1988; *Stephenson and Potter*, 1989].

The polymineralic nature of most rocks adds further complication. Because AMS simultaneously measures the susceptibility of all the minerals in a rock, it will combine the contributions of several different minerals with possibly different orientations. In such situations, the observed AMS does not accurately reflect the preferred orientation of any single mineral. With this complication in mind, *Borradaile* [1988] concluded that the ability of magnetic anisotropy fabrics to reflect finite strain is greatly improved when it can be demonstrated that the measured magnetic anisotropy can be attributed to a single mineral.

The anhysteretic remanent magnetization anisotropy (ARMA) is a technique, first used by *McCabe et al.* [1985], in which only the anisotropy of ferrimagnetic minerals is measured. In this method, an anhysteretic remanent magnetization (ARM) is imparted to a sample using a low (H= 0.1 mT) steady magnetic field superimposed on the alternating field (peak = 30 mT) of an alternating field (AF) demagnetizer. The resulting ARM is measured, and the process is repeated for nine different sample orientations. These nine results are then used to calculate the ARMA tensor following the method of *Girdler* [1961]. Because both the AF and steady magnetic fields used are well below the coercivities of hematite, goethite, and fine-grained pyrrhotite, these minerals will not acquire an ARM. Thus the measured

Paper number 91JB00605.
0148-0227/91/91JB-00605$05.00

ARM and therefore the ARMA can be due to only the magnetic anisotropy of magnetite or coarse-grained pyrrhotite.

This study examines the changes in ARMA with the gradual development of slaty cleavage in the Ordovician Martinsburg Formation observed at the Lehigh Water Gap in eastern Pennsylvania (Figure 1). The shale-to-slate transition in the Martinsburg Formation has been the subject of many studies over the past 100 years [*Chance*, 1882, 1883; *Behre*, 1927; *Broughton*, 1946; *McBride*, 1962; *Drake and Epstein*, 1967; *Epstein and Epstein*, 1969; *Epstein et al.*, 1974; *Holeywell and Tullis*, 1975; *Beutner*, 1978; *Wintsch*, 1978; *Lee et al.*, 1986]. During deformation a strain shadow beneath the more competent Silurian Shawangunk Formation resulted in the preservation of uncleaved Martinsburg Formation (shale) near the Martinsburg-Shawangunk contact [*Holeywell and Tullis*, 1975]. Slaty cleavage develops gradually over a distance (measured horizontally) of 70-130 m south from this contact (Figure 2). The shale displays well-developed bedding which dips 43° to the north (Figure 3*a*). The slaty cleavage is perpendicular to bedding and dips 65° to the south (Figure 3*b*). We also note that a 3-m-wide block of cleaved rock is found 8 m south of the Martinsburg-Shawangunk contact, which is described by *Epstein et al.* [1974] as a subvertical slip cleavage. Corresponding AMS data are presented for comparison with the ARMA results.

SAMPLING AND ANALYSIS

Oriented blocks were collected from 29 sites at regular intervals along a single, continuous outcrop; a schematic diagram of this outcrop and sample locations is shown in Figure 2. All samples were of fine-grained, dark gray shales or slates, except sites Om27, Om29, and Om30, which were coarser-grained sandy slates. Fourteen of the sites are the same samples used by *Housen and van der Pluijm* [1990]; an additional 15 sites were collected for this study. To recover intact blocks, samples were covered with masking tape after marking their orientation; they were then removed and wrapped with additional tape to prevent disintegration of the blocks during transport. In the lab the blocks were first glued together and then coated with nonmagnetic epoxy. The coated blocks were cored with a water-cooled drill; each block yielded 1-10 sample cores. For this study a total of 90 sample cores with 2.5-cm diameter and 2.2-cm length were used. The AMS measurements of the samples from the 15 new sites were made on a Sapphire Instruments (SI-2) susceptibility bridge using the procedures outlined in *Housen and van der Pluijm* [1990].

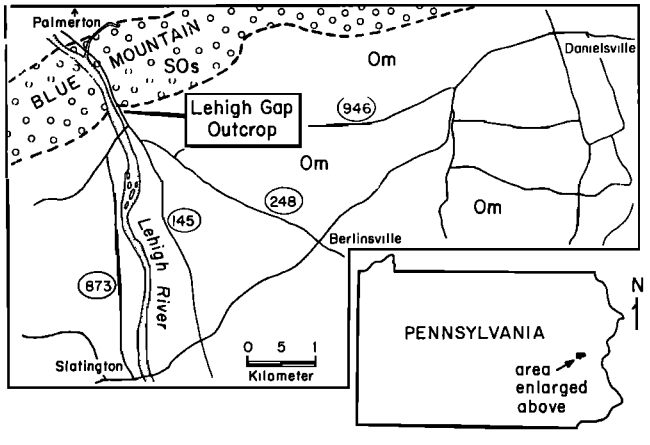

Fig. 1. Location map of the Lehigh Gap outcrop. Highway numbers are shown for reference. The sample site at Lehigh Gap is located above the highway on an abandoned railroad grade and is adjacent to the Appalachian Trail. Om, Ordovician Martinsburg Formation, SOs, Silurian-Ordovician Shawangunk Formation.

For ARMA analysis the samples were first demagnetized with a Schonstedt GSD-1 AF demagnetizer, and a baseline measurement of the remaining (usually less than 0.1 mA/m) sample magnetization was made. The baseline measurement is used to account for any remanent magnetization that cannot be removed by the AF demagnetizer. By means of a DC-powered coil wrapped around the AF demagnetizer coil a steady magnetic field (H= 0.1 mT) was generated. A peak AF value of 30 mT was used to generate the ARM; this value provided the best-resolved ARMA results. Additionally, due to limitations in the design of our DC coil, 30 mT was also the maximum AF that could be used to generate an ARM. The resulting ARM was then measured, and the sample was subsequently demagnetized. Demagnetization between each step was found to remove the generated ARM, restoring the remanence to the baseline value. All ARM measurements were performed with a 2G cryogenic magnetometer in a room isolated from the Earth's magnetic field. The process was repeated for nine sample orientations. The nine ARM results, along with the baseline magnetization measurement, were combined to calculate the ARMA tensor and the orientation and magnitude of the ARMA axes utilizing a computer program developed by *McCabe et al.* [1985] following the method of *Girdler* [1961]. The calculation also tests the assumption that the ARMA results can be described by a triaxial ellipsoid by comparing the observed ARMs for each of the nine sample orientations with the ARMs calculated from the ARMA tensor [see *McCabe et al.*, 1985].

The magnetic mineralogy of these samples was determined by the thermal demagnetization of multicomponent isothermal remanent magnetization (mIRM) developed by *Lowrie* [1990]. This method can identify magnetic minerals by their characteristic coercivities and thermal unblocking temperatures. For this study mIRMs were given to samples using successive application of steady fields of 1.4 T, 0.4 T and 0.1 T in orthogonal directions using an electromagnet. These mIRMs

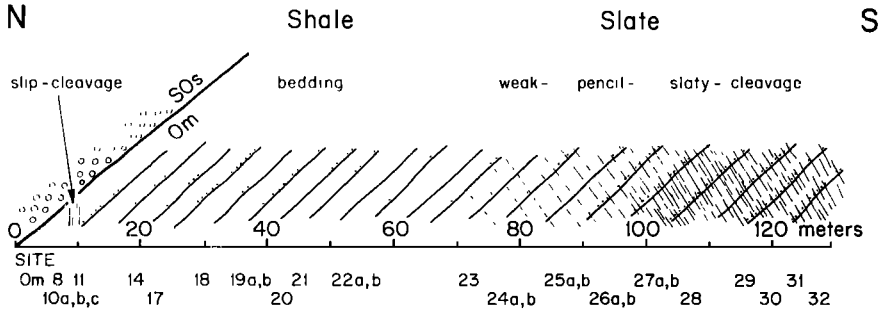

Fig. 2. Schematic diagram of the Lehigh Gap outcrop showing the bedding attitudes and stages of cleavage development. Locations of sample sites (Om8-Om32) and distance in meters from the Martinsburg-Shawangunk contact are marked at the bottom.

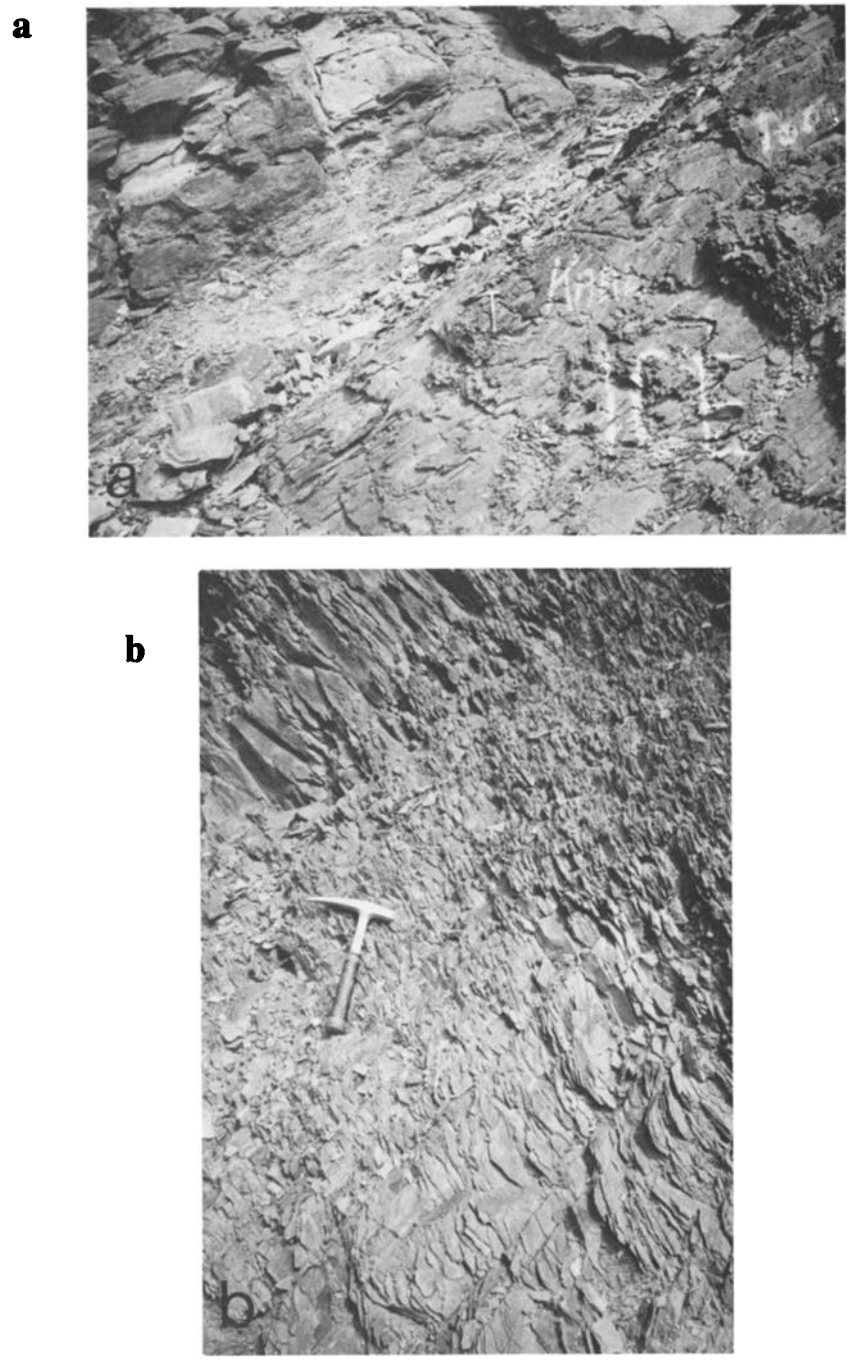

Fig. 3. Field photographs of (*a*) uncleaved Martinsburg Formation shale with bedding dipping 43° to the north and (*b*) well-cleaved slate, with slaty cleavage perpendicular to bedding, dipping 65° to the south.

were then measured, and then the samples were thermally demagnetized. The decay of the mIRMs was measured following each step of the demagnetization process.

RESULTS

Anhysteretic remanent magnetization anisotropy results from the Martinsburg Formation shale-to-slate transition indicate that the ARMA ellipsoid changes in both shape and orientation as slaty cleavage is developed. In Figure 4, lower-hemisphere, equal-area projections of the ARMA axes for each site are shown. Using repeated measurements of single samples and within-site variability, it is estimated that these ARMA orientations are accurate to within 5°. Samples of shale near the Martinsburg-Shawangunk contact display ARMA fabrics dominated by bedding, with the minimum ARMA axis perpendicular to bedding and the maximum and intermediate ARMA axes in the plane of bedding (sites Om8 and Om10, for example). Samples from the well-cleaved portion of this outcrop (sites Om27-Om32) have ARMA fabrics that correspond to the slaty cleavage, with the minimum ARMA axes close to the pole to cleavage, and the maximum and intermediate ARMA axes in the cleavage plane. Samples from the cleaved area near the contact (sites Om10B-Om10C) display ARMA fabrics that correspond to the slip cleavage. In both sets of samples, the maximum ARMA axis generally lies close to the bedding-cleavage intersection. Thus in both the uncleaved and well-

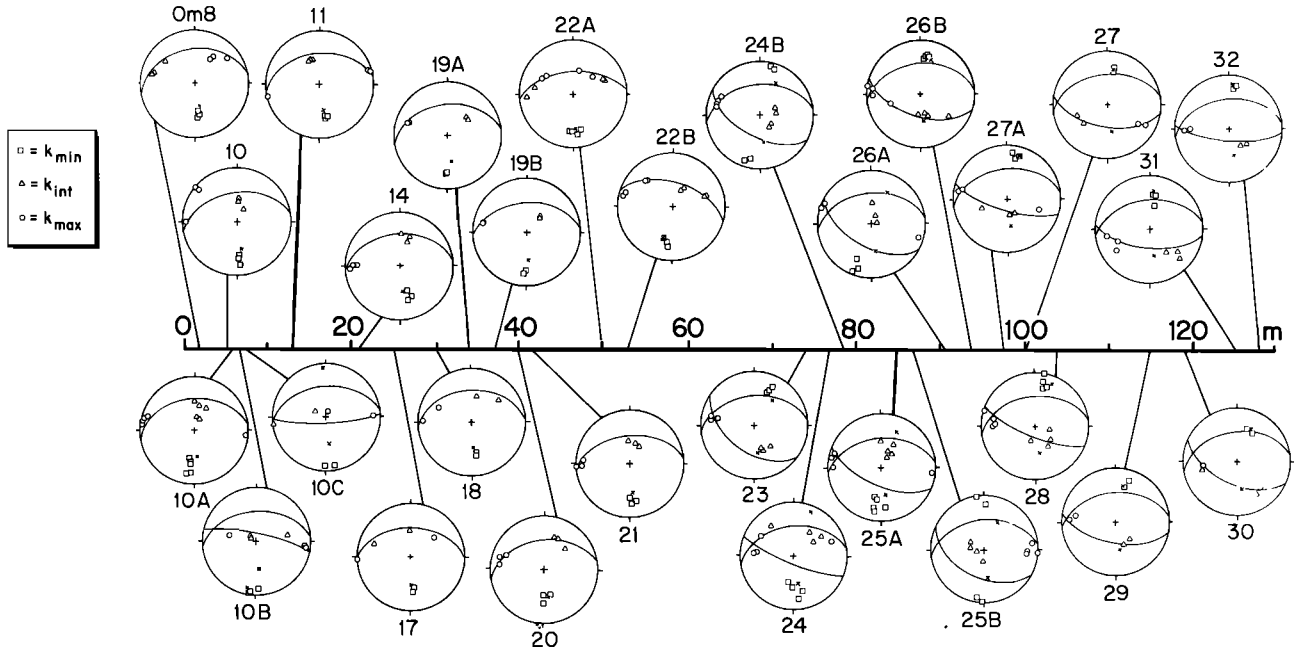

Fig. 4. Equal-area, lower-hemisphere projections of the principal ARMA axes for each site in this study. Bedding planes (north dipping) are shown for the shale samples, both bedding and cleavage (south dipping) planes are shown for the cleaved samples. The horizontal scale is distance in meters from the Martinsburg-Shawangunk contact. Site numbers and their relative locations are indicated.

TABLE 1. Anhysteretic Remanent Magnetization Anisotropy Data

Site	Dist	ARM Axes (mA/m) max	int	min	L	F	%Anis
Om8	2	1.34	1.31	1.16	1.02	1.13	14.21
Om10	6	1.32	1.28	1.16	1.03	1.11	13.28
Om10A	7	1.41	1.34	1.23	1.05	1.10	13.81
Om10B	8	1.88	1.77	1.62	1.07	1.09	14.80
Om10C	9	1.17	1.14	1.07	1.03	1.07	8.88
Om11	13	1.24	1.22	1.08	1.02	1.13	13.42
Om14	21	1.60	1.57	1.43	1.02	1.10	10.94
Om17	25	1.74	1.70	1.54	1.03	1.10	12.39
Om18	30	1.44	1.41	1.25	1.02	1.13	13.90
Om19A	34	1.46	1.43	1.33	1.03	1.07	9.24
Om19B	37	1.61	1.56	1.45	1.03	1.08	10.39
Om20	40	2.48	2.41	2.19	1.03	1.10	12.37
Om21	42	1.63	1.60	1.49	1.02	1.07	9.11
Om22A	50	2.33	2.04	1.74	1.14	1.17	28.97
Om22B	53	3.17	2.85	2.46	1.12	1.17	25.12
Om23	74	5.70	5.43	5.11	1.05	1.06	10.90
Om24	77	1.87	1.78	1.64	1.05	1.08	13.12
Om24B	79	1.46	1.39	1.33	1.05	1.05	9.33
Om25A	85	1.37	1.34	1.28	1.03	1.05	6.77
Om25B	87	1.19	1.15	1.10	1.04	1.04	7.85
Om26A	91	2.49	2.35	2.22	1.05	1.06	11.47
Om26B	94	3.88	3.74	3.04	1.04	1.23	23.64
Om27A	98	2.56	2.46	2.26	1.04	1.10	12.36
Om27 *	100	2.16	2.12	1.98	1.02	1.07	8.74
Om28	104	1.62	1.57	1.48	1.03	1.06	8.82
Om29 *	115	1.54	1.51	1.44	1.02	1.05	7.01
Om30 *	119	5.02	4.88	4.31	1.03	1.13	14.87
Om31	125	31.48	29.87	25.71	1.05	1.16	19.89
Om32	128	1.62	1.57	1.42	1.03	1.10	12.91

Dist is distance in meters from contact. $L=k_{max}/k_{int}$, $F=k_{int}/k_{min}$. %Anis = k_{max}-k_{min}/k_{mean} x100.

ARM axes are magnetization per volume, J (in milliamperes per meter).

* Denotes sand-rich samples

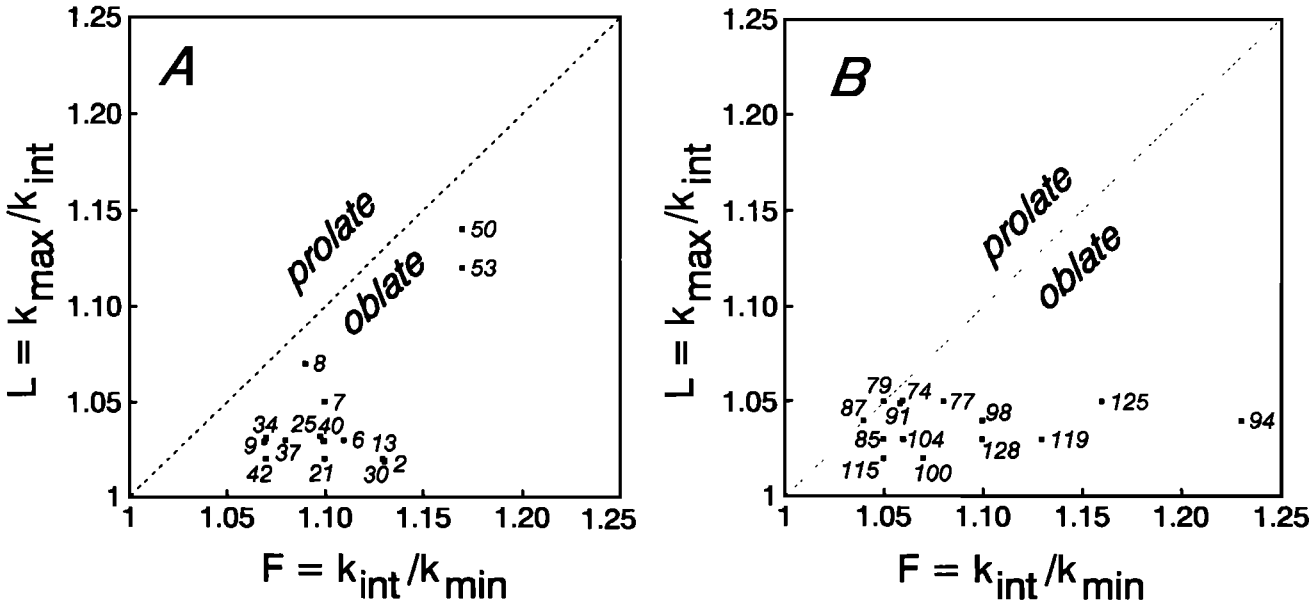

Fig. 5. Flinn diagrams that show the shape of the ARMA ellipsoid for (*a*) shale (2-53) and (*b*) slate (74-128) samples. Results which fall in the oblate field indicate a magnetic foliation; results which fall in the prolate field correspond to magnetic lineations. The distance of each site from the Martinsburg-Shawangunk contact is used as the data marker for that site. Samples from the cleaved block near the contact (8-9) are also included in Figure 5*a*; samples with weak or pencil cleavage (74-91) are shown in Figure 5*b* and lie near the oblate-prolate boundary. See text for discussion.

cleaved samples the ARMA fabric accurately reflects the orientation of the dominant rock fabric. Samples from the area in which cleavage is increasingly developed (sites Om23-Om27A) have ARMA orientations that are not parallel to either bedding or cleavage. These samples are characterized by minimum ARMA axes orientations which fall between those of the shale samples and those of the well-cleaved samples. The significance of this pattern will be further explored in the discussion section.

The shape of the ARMA ellipsoid displays progressive changes along this outcrop. Table 1 lists the magnitudes of the ARMA axes. The parameters L (magnetic lineation), F (magnetic foliation), and percent anisotropy calculated for each site are also given in Table 1. Figure 5 graphically depicts the ARMA ellipsoid shapes in Flinn diagrams, which express the shape of the ARMA ellipsoids by plotting the maximum/intermediate (L) versus the intermediate/minimum (F) ARMA axes. When L is greater than F, the ARMA ellipsoid has a prolate, or elongate, shape. When F is greater than L, the ARMA ellipsoid has a oblate, or flat, shape. The mean shape for each site is plotted using the data from Table 1; the data point for each site is denoted on the plot as the distance (in meters) of that site from the Martinsburg-Shawangunk contact. Figure 5*a* plots the shapes of the ARMA ellipsoids from the uncleaved samples (2-53 m) and shows that the uncleaved samples all display oblate ARMA ellipsoids, with the majority of

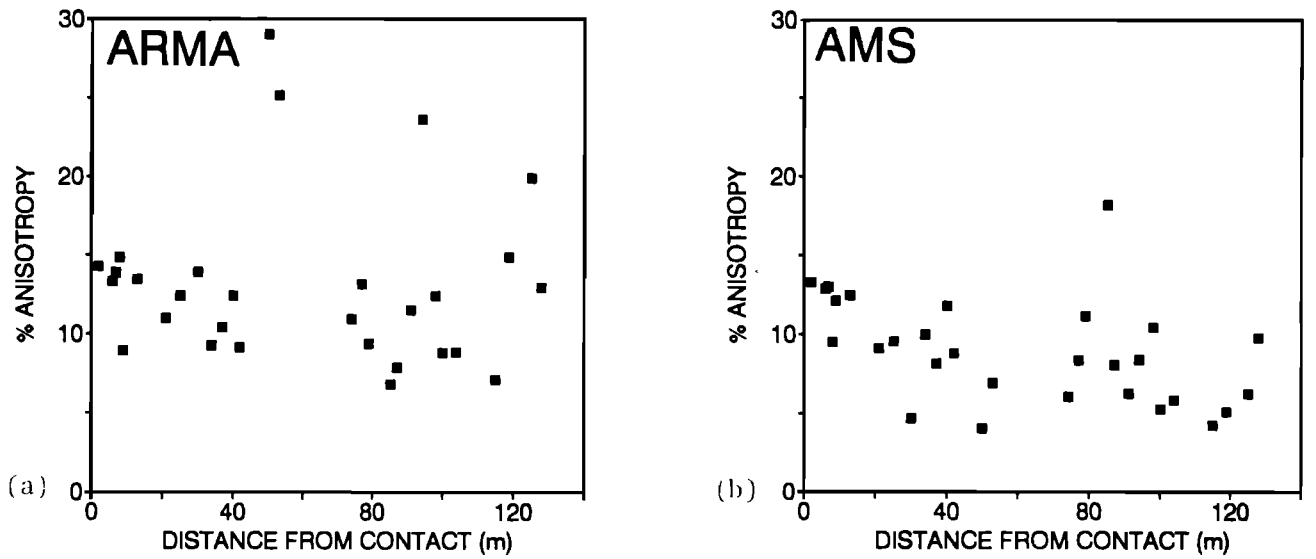

Fig. 6. Plot of (*a*) ARMA and (*b*) AMS percent anisotropy versus distance from the Martinsburg-Shawangunk contact. Percent anisotropy is defined as $((k_{max}-k_{min})/k_{mean})\times 100$ [*Nagata*, 1961]. The majority of samples have values less than 15% and 13% for ARMA and AMS, respectively.

sites having a nearly uniaxial-oblate ($L=1$) shape. The ARMA ellipsoid shapes from the cleaved samples (74-128 m) are shown in Figure 5*b*. Samples having a weak or pencil cleavage (74-91 m) lie near the oblate-prolate boundary of the Flinn diagram, while samples with more pronounced cleavage (94-128 m) have nearly uniaxial-oblate ARMA ellipsoids.

Examination of the percent anisotropy ($\%A=(k_{max}-k_{min}/k_{mean}$) of the ARMA results (Figure 6a) shows no clear pattern relating the degree of anisotropy with cleavage formation. Most samples have anisotropies between 8 and 15 %. Four samples have anisotropies >20 %, but they do not display a discernible relationship to cleavage development.

Characterization of the magnetic mineralogy using mIRM thermal demagnetization experiments [*Lowrie*, 1990] is given in Figure 7, which plots mIRM intensity versus thermal demagnetization temperature. Figure 7*a* is from a representative shale sample; Figure 7*b* is a slate sample. The soft component (H=0.1 T) decays smoothly to zero at a temperature of 550°C, indicating the presence of magnetite. Both plots show no unblocking behavior of the soft component which would indicate the presence of pyrrhotite. Thus the ARM fabrics are attributed to magnetite in these samples.

The AMS results from our previous study [*Housen and van der Pluijm*, 1990] and results from 15 new sites are listed in Table 2. Two AMS orientations were observed; one with k_{max} and k_{int} lying in a plane oriented 20° shallower than bedding in the shale and weakly cleaved slates, the other with k_{max} and k_{int} lying in the cleavage plane in the well-cleaved slates (see Figure 8). Only a few samples deviate from these patterns. As discussed by *Housen and van der Pluijm* [1990] these AMS orientations are identical to the orientation of chlorite basal planes in these rocks. Our new data lend further support to this interpretation. Additional samples from the outcrop that were collected for this study show that the sharp transition between the two AMS fabrics occurs at about 100 m, which is essentially identical to the sharp change in chlorite orientation measured by X ray texture goniometry [compare Figure 8*b* with Figure 6 of *Housen and van der Pluijm*, 1990].

The percent anisotropy from AMS for each site are plotted in Figure 6*b*. The values range from 13 to 4 % and display a slight downward trend in percent anisotropy away from the Shawangunk Formation contact. One site, Om25A, has an anomalously high value of 18 %. As with the ARMA results, no clear relationship between AMS percent anisotropy and the development of cleavage is observed.

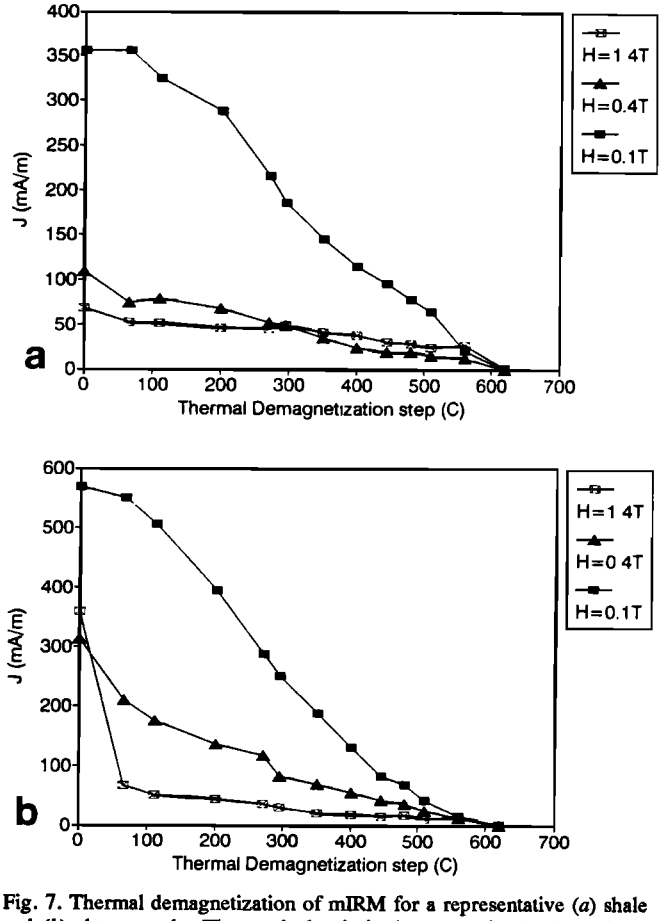

Fig. 7. Thermal demagnetization of mIRM for a representative (*a*) shale and (*b*) slate sample. The vertical axis is the magnetization intensity J (in milliamperes per meter), and the horizontal axis is the temperature used during progressive thermal demagnetization of the mIRM. The hard (H = 1.4 T) mIRM component is denoted by open squares, the medium (H = 0.4 T) by triangles, and the soft (H = 0.1 T) by solid squares. The coercivity of the soft component would magnetize (titano)magnetite or coarse-grained pyrrhotite. The observed unblocking temperature (T > 550° C) indicates that the soft-coercivity mineral in these rocks is magnetite [*Lowrie*, 1990].

DISCUSSION

There has been much debate among geologists during the past 150 years on the mechanism of cleavage formation (see reviews by *Harker* [1885], *Siddans* [1972], *Wood* [1974], *Williams* [1977], *Engelder and Marshak* [1985]). Paralleling this debate, although over a much shorter time span, has been the discussion raised by the many attempts to quantitatively link magnetic anisotropy and finite strain in slates [*Owens*, 1974; *Singh et al.*, 1975; *Hrouda*, 1976, 1987; *Kligfield et al.*, 1977; *Rathore*, 1979, 1988; *Rochette and Vialon*, 1984; *Hirt et al.*, 1988; *Borradaile and Sarvas*, 1990]. The crucial problem in these correlations lies in the assumptions made for the mechanism of cleavage formation. In most models it is assumed that the magnetic anisotropy carriers undergo passive rotation during cleavage formation and that the changes in the preferred orientation of these minerals can be quantified by a rotational, March strain model [see *Owens*, 1974].

Examination of the ARMA results shows that the orientation of the minimum ARMA axes (k_{min}) progresses in orientation from perpendicular to bedding in the uncleaved shale, to orientations between the poles to bedding and cleavage in samples with weak or pencil cleavage, to orientations perpendicular to cleavage in the well-cleaved samples (Figure 4). This trend indicates that magnetite is oriented parallel to the dominant rock fabric in the shale and slate end-member samples, i.e., parallel to bedding and cleavage, respectively. The cleavage in the block near the Martinsburg-Shawangunk contact is also reflected in the ARMA fabric. The significance of the intermediate orientations found in the weakly cleaved samples in terms of the possible use of ARMA as a strain marker using rotational models are discussed below.

Microstructural studies of the shale-to-slate transition in the Martinsburg Formation have indicated that cleavage formation was accompanied by dissolution and neocrystallization of chlorite and mica [*Holeywell and Tullis*, 1975; *Wintsch*, 1978; *Wright and Platt*, 1982; *Lee et al.*, 1986]. Our AMS fabrics from the Martinsburg Formation closely mimic the orientation of chlorite in this outcrop, which, combined with the agreement between the observed susceptibility magnitudes and those reported for chlorite by *Borradaile et al.* [1987], indicate that low-field susceptibility is controlled primarily by paramagnetic chlorite. *Housen and van der Pluijm* [1990] concluded that the

TABLE 2. Anisotropy of Magnetic Susceptibility Data

Site	Dist	Susceptibility Axes (1×10^{-4} SI units) k_{max}	k_{int}	k_{min}	L	F	%Anis
Om8	2	2.31	2.26	2.01	1.02	1.12	13.25
Om10	6	3.80	3.64	3.34	1.05	1.09	12.83
Om10A	7	3.57	3.40	3.14	1.05	1.08	12.93
Om10B	8	3.18	3.01	2.89	1.06	1.04	9.47
Om10C	9	3.20	3.02	2.84	1.06	1.06	12.07
Om11	13	3.27	3.19	2.88	1.03	1.11	12.42
Om14	21	2.81	2.75	2.57	1.02	1.07	9.04
Om17	25	3.11	3.02	2.83	1.03	1.07	9.52
Om18	30	2.42	2.37	2.31	1.02	1.03	4.65
Om19A	34	3.21	3.13	2.90	1.03	1.08	9.96
Om19B	37	3.18	3.11	2.93	1.02	1.06	8.15
Om20	40	3.75	3.64	3.33	1.03	1.10	11.76
Om21	42	3.17	3.09	2.91	1.03	1.06	8.74
Om22A	50	1.79	1.77	1.72	1.01	1.03	4.01
Om22B	53	2.71	2.62	2.53	1.03	1.04	6.85
Om23	74	2.61	2.52	2.46	1.04	1.03	6.03
Om24	77	3.57	3.45	3.29	1.03	1.05	8.31
Om24B	79	2.33	2.26	2.09	1.03	1.09	11.12
Om25A	85	3.08	2.75	2.57	1.12	1.07	18.20
Om25B	87	2.80	2.70	2.58	1.03	1.05	8.03
Om26A	91	2.53	2.45	2.38	1.03	1.03	6.21
Om26B	94	2.02	1.94	1.86	1.04	1.05	8.37
Om27A	98	2.23	2.13	2.01	1.05	1.06	10.45
Om27 *	100	2.43	2.39	2.30	1.02	1.04	5.26
Om28	104	2.78	2.71	2.62	1.03	1.03	5.84
Om29 *	115	2.63	2.59	2.52	1.01	1.03	4.22
Om30 *	119	2.46	2.44	2.34	1.01	1.04	5.11
Om31	125	3.22	3.12	3.02	1.03	1.03	6.23
Om32	128	2.72	2.55	2.47	1.07	1.03	9.74

Dist is distance in meters from contact. $L = k_{max}/k_{int}$, $F = k_{int}/k_{min}$. $\%Anis = k_{max}\text{-}k_{min}/k_{mean} \times 100$.

* Denotes sand-rich samples

observed new growth of chlorite during cleavage formation invalidated March strain models that correlate AMS and finite strain in these slates. This conclusion is supported by measurements of magnetic hysteresis [M. Jackson, written communication 1989], which indicate that greater than 90 % of the low-field susceptibility is due to paramagnetic sources in these rocks.

The orientations of the ARMA fabrics in this outcrop, along with the AMS fabrics, are shown in Figure 8. Orientations are plotted as rakes on a reference plane whose pole is the bedding-cleavage intersection (Figure 8*a*); AMS and ARMA orientations are defined by the plane containing the maximum and intermediate susceptibility axes. The patterns are plotted as a function of distance from the Martinsburg-Shawangunk contact (Figure 8*b*). As previously discussed, ARMA orientations are parallel to the dominant rock fabric in the shale and slate portions of the outcrop and intermediate to bedding and cleavage in the weak and pencil cleavage samples. A smooth progression from bedding-parallel to cleavage-parallel, however, is not observed. In contrast, AMS results have only two orientations, one at a small angle to bedding, the other roughly parallel to cleavage. No AMS orientations intermediate to bedding and cleavage were observed. Samples from the cleaved block near the Martinsburg-Shawangunk contact (Om10B-Om10C) have AMS orientations which seem to have been affected by, but are not parallel to, this cleavage. ARMA results from this block are, however, nearly parallel to this cleavage. The anomalous orientation of the AMS results from sample Om22A (50 m) is attributed to the isotropic contribution of 1- to 2-mm pyrite cubes present in these samples. This comparison between ARMA and AMS orientations in Figure 8*b* clearly demonstrates that ARMA is a more reliable indicator of the dominant rock fabrics in the Martinsburg Formation.

There are two possible explanations for the intermediate ARMA orientations observed in the weak and pencil cleavage samples (74-94 m). The first explanation is that magnetite has rotated from bedding-parallel to cleavage-parallel orientations with increasing degree of cleavage development. The absence of a smooth transition in ARMA orientations between end-member bedding and cleavage fabrics would be explained by heterogeneous deformation in these rocks. The second explanation is that magnetite growth has occurred during cleavage formation. This possibility requires that magnetite (re)crystallized in an orientation parallel to cleavage, not unlike the behavior of chlorite and mica. Consequently, the measured ARMA tensor would be a composite of two ARMA fabrics, one from magnetite parallel to bedding, the other from second-generation magnetite parallel to cleavage. Magnetite parallel to cleavage becomes the dominant control on the ARMA fabric when its proportion exceeds that of magnetite parallel to bedding, as is the case with the well-cleaved samples. In the weakly cleaved samples the two populations of magnetite are nearly equal in proportion, thus small variations in the relative abundances of each population will greatly affect ARMA orientations. The latter process would account for the variable ARMA orientations in the weakly cleaved samples. The ARM

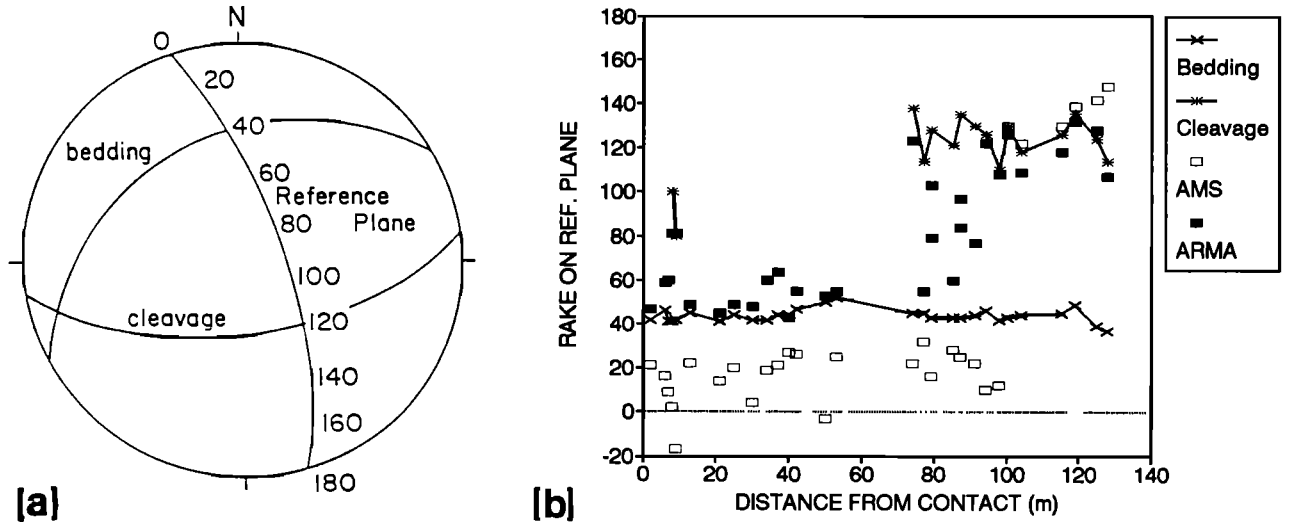

Fig. 8. Orientations of bedding, cleavage, AMS, and ARMA fabrics. (*a*) Reference plane against which orientations are plotted. The pole to the reference plane is the bedding-cleavage intersection. Planar orientations are plotted as rakes on this reference plane; as shown here, bedding has a rake of 40° and cleavage has a rake of 120°. (*b*) Plot of bedding, cleavage, AMS, and ARMA orientations as a function of distance from the Martinsburg-Shawangunk contact. The vertical axis is the rake on the reference plane, the horizontal axis is the distance in meters from the contact. AMS and ARMA orientations are represented by the plane containing the maximum and intermediate susceptibility axes. ARMA orientations are parallel to the dominant rock fabrics in the shale and well-cleaved slate samples. Weak and pencil cleavage samples display orientations in between those of bedding and cleavage. AMS shows only two orientations, one about 20° shallower than bedding, the other roughly parallel to cleavage; no intermediate AMS orientations are observed.

intensities and low-field susceptibilities for these samples do not show any increase in magnitude (with the exception of Om31) which would indicate addition of new magnetite with cleavage formation. New magnetite must thus be derived from the dissolution of preexisting magnetite in these rocks.

The shape of the ARMA ellipsoids display a characteristic progression from shale to slate (Figure 9). Shale samples are characterized by uniaxial-oblate ARMA ellipsoids with the planes of flattening parallel to the bedding planes. Samples exhibiting pencil cleavage have ARMA ellipsoid shapes that plot at the prolate-oblate boundary, with the elongation direction parallel to the bedding-cleavage intersection. Well-cleaved samples display strongly uniaxial-oblate ARMA ellipsoid shapes. This trend from oblate to prolate then back to oblate shapes can be explained by the presence of two contributing magnetite populations, i.e., the original bedding fabric and the secondary cleavage fabric. Both the shale and slate samples have well-developed uniaxial-oblate ARMA ellipsoids, but their short axes are approximately perpendicular to each other. Superimposing these shale and slate ellipsoids results in a shape that will trend to the prolate field as the relative contributions of the two ellipsoids approach equality. This ARMA fabric is seen in the weakly cleaved and pencil slates. As the cleavage fabric becomes dominant, the ARMA ellipsoid shape will trend back to the uniaxial-oblate field as seen in Figure 9. These well-cleaved samples do not display a strong magnetic lineation (Table 1). Examination of Figure 4 shows that the position of k_{max} measured by ARMA consistently lies at the bedding-cleavage intersection in not only the cleaved samples, but in some of the shale samples as well. Superposition of the two uniaxial-oblate ellipsoids as described above would produce k_{max} orientations parallel to the bedding-cleavage intersection and account for the lack of a strong magnetic lineation. We add, however, that this trend in the shapes of the ARMA ellipsoid can also be produced by rotation of existing magnetite grains. This trend in ellipsoid shapes cannot therefore be used to discriminate between rotation or (re)crystallization of magnetite.

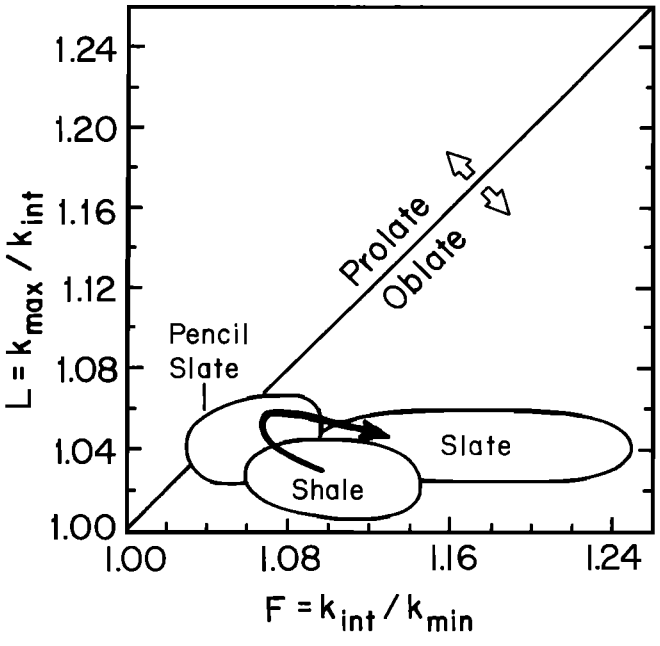

Fig. 9. Summary Flinn diagram, showing ARMA ellipsoid shapes for shale, weak cleavage (pencil slate), and well-cleaved slate samples. ARMA ellipsoids trend from an initial, uniaxial-oblate shape in the shale to the oblate-prolate boundary in the pencil slates to strongly oblate shapes in the slates.

CONCLUSIONS

Analysis of magnetic anisotropy fabrics in the shale-to-slate transition of the Martinsburg Formation at Lehigh Gap reveals that ARMA, which measures only the preferred orientation of magnetite, strongly reflects the dominant rock fabric. Observed ARMA orientations intermediate to bedding and cleavage, found in samples with a weakly developed cleavage, may have arisen

from two possible mechanisms: (1) passive rotation of magnetite from bedding-parallel to cleavage-parallel with the progressive formation of slaty cleavage, requiring highly heterogeneous deformation, or (2) dissolution and new growth of magnetite during cleavage formation, resulting in composite ARMA fabrics of bedding-parallel and cleavage-parallel magnetite. Visual characterization of magnetite behavior is necessary to distinguish between either interpretation.

Dissolution and new growth of paramagnetic minerals such as chlorite, and the effect of compositional changes commonly seen in sediments (e.g., the addition of pyrite) both result in AMS fabrics that do not reflect the dominant rock fabric in these samples. Such changes in AMS fabrics clearly demonstrate the shortcomings in correlations of AMS with finite strain.

In contrast to AMS, ARMA appears to be very sensitive to changes in the rock fabric, such as those resulting from deformation. Thus ARMA is more suitable to the study of deformed rocks.

Acknowledgments. Research was supported by the National Science Foundation, grant EAR-8903805, and the University of Michigan Scott Turner Fund. We thank M. Jackson for discussion and comments, and for measurements of hysteresis loops carried out at the University of Minnesota. Beth Housen is thanked for her able assistance in the field. R. Van der Voo, R. Molina-Garza, R. Johnson, C. Richter, and reviewers A. Hirt and K. Kodama provided helpful comments and suggestions.

REFERENCES

Behre, C.H., Slate in Northampton County, Pennsylvania, Pa. Geol. Surv., 4th ser., *Bull. M9*, 308 pp. Harrisburg, 1927.

Beutner, E.C., Slaty cleavage and related strain in Martinsburg slate, Delaware Water Gap, New Jersey, *Am. J. Sci., 278*, 1-23, 1978.

Borradaile, G.J., Anisotropy of magnetic susceptibility: rock composition versus strain, *Tectonophysics, 138*, 327-329, 1987.

Borradaile, G.J., Magnetic susceptibility, petrofabrics and strain, *Tectonophysics, 156*, 1-20, 1988.

Borradaile, G.J., and C. Alford, Relationship between magnetic susceptibility and strain in laboratory experiments, *Tectonophysics, 133*, 121-135, 1987.

Borradaile, G.J., and C. Alford, Experimental shear zones and magnetic fabrics, *J. Struct. Geol., 10*, 895-904, 1988.

Borradaile, G.J., and J.S. Mothersill, Coaxial deformed and magnetic fabrics without simply correlated magnitudes of principal values, *Phys. Earth Planet. Inter., 35*, 294-300, 1984.

Borradaile, G.J., and P. Sarvas, Magnetic susceptibility fabrics in slates: structural, mineralogical and lithological influences, *Tectonophysics, 172*, 215-222, 1990.

Borradaile, G.J., and D.H. Tarling, The influence of deformation mechanisms on magnetic fabrics in weakly deformed rocks, *Tectonophysics, 77*, 151-168, 1981.

Borradaile, G.J., J. Mothersill, D. Tarling, and C. Alford, Sources of magnetic susceptibility in a slate, *Earth Planet. Sci. Lett., 76*, 336-340, 1986.

Borradaile, G.J., W. Keeler, C. Alford, and P. Sarvas, Anisotropy of magnetic susceptibility of some metamorphic minerals, *Phys. Earth Planet. Inter., 48*, 161-166, 1987.

Bossart, P., R. Ottiger, F. Heller, Rock magnetic properties and structural development in the core of the Hazra-Kashmir syntaxis, NE Pakistan, *Tectonics, 9*, 103-121, 1990.

Broughton, J.G., An example of the development of cleavages, *J. Geol., 54*, 1-18, 1946.

Chance, H.M., Special survey of the Lehigh water gap, in White, I.C., The geology of Pike and Monroe Counties, Pa. Geol. Surv., 2nd surv., *Rept. G6*, pp. 349-363, Harrisburg, 1882.

Chance, H.M., The slate quarries in 1875, with four cross sections, in Prime, F.,Jr., The geology of Lehigh and Northampton Counties, Pa. Geol. Surv., 2nd surv., *Rept. D3*, vol. 1, pp. 148-160, Harrisburg, 1883.

Cogne, J.P., and H. Perroud, Anisotropy of magnetic susceptibility as a strain gauge in the Flamanville granite, NW France, *Phys. Earth Planet. Inter., 51*, 264-270, 1988.

Drake, A.A., and J.B. Epstein, The Martinsburg Formation (middle and upper Ordovician) in the Delaware Valley, Pennsylvania-New Jersey, *U.S. Geol. Surv. Bull. 1244-H*, 16 pp., 1967.

Engelder, T., and S. Marshak, Disjunctive cleavage formed at shallow depths in sedimentary rocks, *J. Struct. Geol., 7*, 327-343, 1985.

Epstein, J.B., and A.G. Epstein, Geology of the Valley and Ridge province between Delaware Water Gap and Lehigh Gap, Pennsylvania, in *Geology of Selected Areas in New Jersey and Eastern Pennsylvania, and Guidebook of Excursions*, edited by S. Subitzky, pp. 132-205, Rutgers University Press, New Brunswick, N.J., 1969.

Epstein, J.B., W.D. Sevon, J.D. Glaeser, Geology and mineral resources of the Lehighton and Palmerton quadrangles, Carbon and Northampton counties, Pennsylvania, Pa. Geol. Surv., 4th ser., *Atlas 195c and 195d*, 460 pp., Harrisburg, 1974.

Fuller, M.D., Magnetic anisotropy and paleomagnetism, *J. Geophys. Res., 68*, 293-309, 1963.

Girdler, R.W., The measurement and computation of anisotropy of magnetic susceptibility of rocks, *Geophys. J. R. Astron. Soc., 5*, 34-44, 1961.

Goldstein, A.G. and L.L. Brown, Magnetic susceptibility anisotropy of mylonites from the Brevard Zone, North Carolina, U.S.A., *Phys. Earth Planet. Inter., 51*, 290-300, 1988.

Graham, J.W., Magnetic susceptibility anisotropy, an unexploited petrofabric element, *Geol. Soc. Am. Bull., 65*, 1257-1258, 1954.

Harker, A., On slaty cleavage and allied rock-structures, with special reference to the mechanical theories of their origin, *Rep. British Assoc. Adv. Sci., 1885 meeting*, 813-852, 1885.

Henry, B., Magnetic fabric and orientation tensor of minerals in rocks, *Tectonophysics, 165*, 21-27, 1989.

Henry, B., and L. Daly, From qualitative to quantitative magnetic anisotropy analysis: the prospect of finite strain calibration, *Tectonophysics, 98*, 327-336, 1983.

Hirt, A.M., W. Lowrie, W.S. Clendenen, and R. Kligfield, The correlation of magnetic anisotropy with strain in the Chelmsford Formation of the Sudbury Basin, Ontario, *Tectonophysics, 145*, 177-189, 1988.

Holeywell, R.C., and T.E. Tullis, Mineral reorientation and slaty cleavage in the Martinsburg Formation, Lehigh Gap, Pennsylvania, *Geol. Soc. Am. Bull., 86*, 1296-1304, 1975.

Housen, B.A., and B.A. van der Pluijm, Chlorite control of correlations between strain and anisotropy of magnetic susceptibility, *Phys. Earth Planet. Inter., 61*, 315-323, 1990.

Hrouda, F., The origin of cleavage in the light of magnetic anisotropy investigations, *Phys. Earth Planet. Inter., 13*, 132-142, 1976.

Hrouda, F., Magnetocrystalline anisotropy of rocks and massive ores: a mathematical model study and its fabric implications, *J. Struct. Geol., 2*, 459-462, 1980.

Hrouda, F., Mathematical model relationship between the paramagnetic anisotropy and strain in slates, *Tectonophysics, 142*, 323-327, 1987.

Hrouda, F., and R. Lanza, Magnetic fabric in the Biella and Traversella stocks (Periadriatic Line): implications for the mode of emplacement, *Phys. Earth Planet. Inter., 56*, 337-348, 1989.

Hrouda, F., S. Jacko, and J. Hanak, Parallel magnetic fabrics in metamorphic, granitoid and sedimentary rocks of the Branisko and Cierna hora Mountains (E Slovakia) and their tectonometamorphic control, *Phys. Earth Planet Inter., 51*, 271-289, 1988.

Jackson, M., D. Sprowl, and B. Ellwood, Anisotropies of partial anhysteretic remanence and susceptibility in compacted black shales: grainsize- and composition-dependent magnetic fabric, *Geophys. Res. Lett., 16*, 1063-1066, 1989.

Johns, M.K., M. Jackson, J. Marvin, S. Banerjee, and P. Hudleston, Magnetic anisotropy: the role of compositional variation in synthetic and natural samples, *Eos Trans. AGU, 71*, 492, 1990.

Jover, O., P. Rochette, J.P. Lorand, M. Maeder, and J.L. Bouchez, Magnetic mineralogy of some granites from the French Massif Central: origin of their low-field susceptibility, *Phys. Earth Planet. Inter., 55*, 79-92, 1989.

Kligfield, R.. Lowrie, W. and Dalziel, I., Magnetic susceptibility anisotropy as a strain indicator in the Sudbury Basin, Ontario, *Tectonophysics, 40*, 287-308, 1977.

Lee, J.H., D.R. Peacor, D. Lewis, and R.P. Wintsch, Evidence for syntectonic crystallization for the mudstone to slate transition at Lehigh Gap, Pennsylvania, U.S.A., *J. Struct. Geol., 8*, 767-780, 1986.

Lowrie, W., Identification of ferromagnetic minerals in a rock by coercivity and unblocking temperature properties, *Geophys. Res. Lett., 17*, 159-162, 1990.

McBride, E.F., Flysch and associated beds of the Martinsburg Formation (Ordovician), central Appalachians, *J. Sediment. Petrol., 32,* 39-91, 1962.

McCabe, C., M. Jackson, and B. Ellwood, Magnetic anisotropy in the Trenton limestone: results of a new technique, anisotropy of anhysteretic susceptibility, *Geophys. Res. Lett., 12,* 333-336, 1985.

Nagata, T., *Rock Magnetism,* 350 pp, Maruzen, Tokyo, 1961.

Owens, W.H., Mathematical model studies on factors affecting the magnetic anisotropy of deformed rocks, *Tectonophysics, 24,* 115-131, 1974.

Pearce, G.W., and F. Fueten, An intensive study of magnetic susceptibility anisotropy of amphibolite layers of the Thompson Belt, North Manitoba, *Tectonophysics, 162,* 315-329, 1989.

Potter, D.K., and A. Stephenson, Single-domain particles in rocks and magnetic fabric analysis, *Geophys. Res. Lett., 15,* 1097-1100, 1988.

Rathore, J.S., Magnetic susceptibility anisotropy in the Cambrian Slate Belt of North Wales and correlation with strain, *Tectonophysics, 53,* 83-97, 1979.

Rathore, J.S., Strain to anisotropy correlations corrected for the Digico calibration error, *Phys. Earth Planet. Inter., 51,* 355-360, 1988.

Rochette, P., Magnetic susceptibility of the rock matrix related to magnetic fabric studies, *J. Struct. Geol., 9,* 1015-1020, 1987.

Rochette, P., Inverse magnetic fabric in carbonate-bearing rocks, *Earth Planet. Sci. Let., 90,* 229-237, 1988.

Rochette, P., and P. Vialon, Development of planar and linear fabrics in Dauphinois shales and slates (French Alps) studied by magnetic anisotropy and its mineralogical control, *J. Struct. Geol., 6,* 33-38, 1984.

Siddans, A.W.B., Slaty cleavage- a review of research since 1815. *Earth Sci. Rev., 8,* 205-232, 1972.

Singh, J. (now Rathore, J.), D.J. Sanderson, and D.H. Tarling, The magnetic susceptibility anisotropy of deformed rocks from North Cornwall, England, *Tectonophysics, 27,* 141-153, 1975.

Stephenson, A., and D.K. Potter, Some aspects of the measurement of magnetic anisotropy, in *Geomagnetism and Paleomagnetism,* edited by F.J. Lowes et al., pp. 271-278, Kluwer Academic, Boston, Mass., 1989.

Uyeda, S., M.D. Fuller, J.C. Belshe, and R.W. Girdler, Anisotropy of magnetic susceptibility of rocks and minerals, *J. Geophys. Res., 68,* 279-291, 1963.

Vetter, J.R., K.P. Kodama, and A. Goldstein, Reorientation of remanent magnetism during tectonic fabric development: an example from the Waynesboro Formation, Pennsylvania, U.S.A., *Tectonophysics, 165,* 29-39, 1989.

Williams, P.F., Foliation: a review and discussion, *Tectonophysics, 39,* 305-328, 1977.

Wintsch, R.P., A chemical approach to the preferred orientation of mica, *Geol. Soc. Am. Bull., 89,* 1715-1718, 1978.

Wood, D.S., Current views of the development of slaty cleavage, *Annu. Rev. Earth Planet. Sci., 2,* 369-401, 1974.

Wood, D.S., G. Oertel, J. Singh, and M.F. Bennet, Strain and anisotropy in rocks, *Philos. Trans. R. Soc. London, Ser. A, 283,* 78-80, 1976.

Wright, T.O., and L.B. Platt, Pressure dissolution and cleavage in the Martinsburg shale, *Am. J. Sci., 282,* 122-135, 1982.

B.A. Housen and B.A. van der Pluijm, Department of Geological Sciences, 1006 C.C. Little Building, University of Michigan, Ann Arbor, MI 48109-1063

(Received September 21, 1990;
revised February 19, 1991;
accepted February 26, 1991.)